Initial Rupture Processes of the 2006 Pingtung Earthquake from near Source Strong-Motion Records

Bor-Shouh Huang[1,*], Yi-Ling Huang[2], Shiann-Jong Lee[1], Yue-Gau Chen[3], and Juen-Shi Jiang[4]

[1] *Institute of Earth Sciences, Academia Sinica, Nankang, Taipei, Taiwan, ROC*
[2] *Institute of Applied Geosciences, National Taiwan Ocean University, Keelung, Taiwan, ROC*
[3] *Department Geosciences, National Taiwan University, Taipei, Taiwan, ROC*
[4] *Seismological Center of Central Weather Bureau, Taipei, Taiwan, ROC*

ABSTRACT

The magnitude 7.1 Pingtung offshore earthquake occurred on 26 December 2006 at a depth of 40 - 60 km within the subduction zone of the Eurasian plate. This event exhibits an emergent onset. The first large amplitude arrivals were delayed by several seconds with respect to the origin time and were preceded by small-scale slip. This event is one of a few large intermediate depth earthquakes well recorded in a near source region. Based on beamforming analysis, some near source recordings were used in this study to investigate the initial rupture process of this event. Analyzed results indicate that initial fault rupture of this event at the hypocenter was of short duration with initial resultant fault slip extending southward toward the shallower portion of the fault plane. Thereafter, a detected rupture front propagated both northward and downward. Following small-scale initial slip, a major rupture arose. A detailed rupture process has been reconstructed using backward projection of array seismograms from the fault plane to image fault slip. The spatial and temporal evolution of initial onset presents the same rupture behavior determined by beamforming analysis. Our analysis appears to indicate the distinct possibility of an initial seismic nucleation phase; however, uncertainties remain and a cascade process cannot be ruled out completely.

Key words: Pingtung earthquake, Beamforming, Initial slip, Rupture process
Citation: Huang, B. S., Y. L. Huang, S. J. Lee, Y. G. Chen, and J. S. Jiang, 2008: Initial rupture processes of the 2006 Pingtung earthquake from near source strong-motion records. Terr. Atmos. Ocean. Sci., 19, 547-554, doi: 10.3319/TAO.2008.19.6.547(PT)

1. INTRODUCTION

On 26 December 2006, two closely timed earthquakes of magnitudes (M_w) 7.1 and 6.9 occurred at intermediate depths offshore southwestern Taiwan. The first earthquake occurred at 1226 UTC; the epicenter was located at 21.67°N and 120.56°E [Central Weather Bureau (CWB) catalogue] with a focal depth of 44 km. It was followed by another earthquake eight minutes later at 21.97°N and 120.42°E, about 36 km to the north-northeast of the first shock with a focal depth of 50 km (Fig. 1). This earthquake sequence caused 44 injuries, including 2 fatalities, 3 building collapses, and the rupture of submerged communications cables, resulting in significant economic loss (National Disaster Prevention and Protection Commission, ROC 2007).

Both events, known as the 2006 twin Pingtung offshore earthquakes, occurred within a transition zone along the north-south trending boundary between the Eurasian plate and Philippine Sea plate. The normal-faulting focal mechanism of the first shock suggests that it occurred as a result of intraplate stresses within the subducting Eurasian plate. The second shock was determined to be right-lateral strike-slip faulting on a northeast striking fault or left-lateral faulting on a north-northwest striking fault (Global CMT Solution). Historically, this region has low seismicity. The twin earthquakes were the biggest events to have occurred to the west of the Hengchun Peninsula in the past 40 years. The subsequent aftershocks determined by the Central Weather Bureau Seismic Network (CWBSN) were distributed in a north-northwest trend with depths mostly from 20 to 60 km (Fig. 1).

The first event has an emergent onset. Seismograms recorded by strong motion and broadband instruments at local

---

* Corresponding author
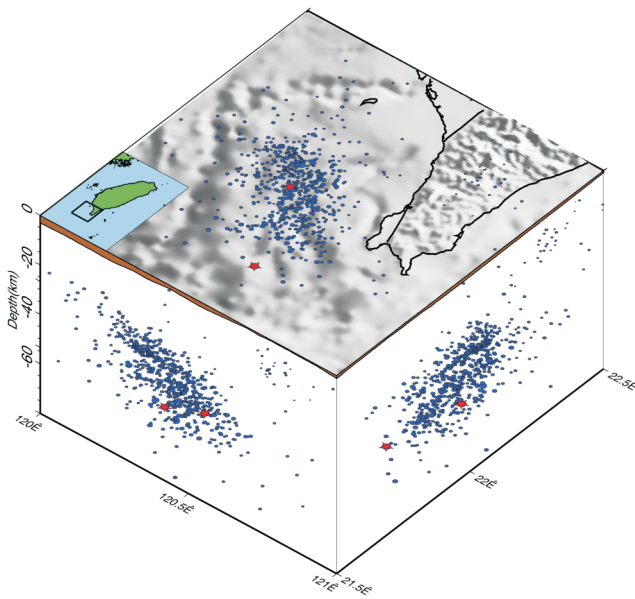 E-mail: hwbs@earth.sinica.edu.tw

Fig. 1. Distribution of aftershocks of the Pingtung earthquake sequence reported by CWBSN. Stars show the locations of the twin events.

distances all show several seconds of arrivals of small but increasing amplitude followed by the onset of a primary energy release. Similar observations have been reported from other large earthquakes (Choy and Dewey 1988; Haessler et al. 1992; Abercrombie and Mori 1994); however, this event is one of a few large intermediate depth earthquakes well recorded in a near source region by a dense local strong motion network, i.e., the CWB strong motion seismic network (Shin 1993; Liu et al. 1999). These nearby dense seismic recordings provided us an opportunity to investigate the initial rupture behaviors of a large earthquake.

In this study, near source dense seismic network recordings were used to investigate the spatial relationship between the hypocenter and the onset of a large energy release. A beamforming method was applied to estimate the azimuth of approach and apparent velocity of the incoming P wave (Goldstein and Archuleta 1991) and deduce the rupture propagation within the fault plane. Our analysis presents an example of the spatial and temporal evolution of a large earthquake in its initial stage. We identify relative locations of seismic energy releases in the first few seconds after its rupture initiation and analyze its detailed onset properties. Our results can be used for further study of the entire rupture process, and provide fundamental information on nucleation and early growth of large earthquakes.

2. DATA

The Pingtung earthquake sequence was well recorded by the CWB strong motion seismic network in southern Taiwan (Fig. 2). This data set represents near source strong

ground motion observations for the study of source rupture and wave propagation. In this study, near source seismic observations from the Hengchun Peninsula were examined. All seismograms had high signal to noise ratios; and also S wave arrivals were always more than 5 seconds later than initial P wave arrivals, providing an unpolluted signal window for direct observation of the fault rupture in its initial stage. All data were recorded by digital accelerometers operated in trigger mode, and most instruments were equipped with GPS clocks to provide absolute timing. Unfortunately, some data lost their GPS signals. However, it was found that all seismograms started before initial arrivals, providing an opportunity to correct relative timing among seismograms. The data were carefully corrected and a common time base was constructed using the method developed by Huang (2000). We corrected onset timings for records without absolute timing by assuming the earthquake initiated at the hypocenter reported by CWB. After correction, it was expected that time errors would be consistently less than 0.2 sec (Huang 2000). Furthermore, one station (TWKB) of the Broadband Array in Taiwan for Seismology (BATS) is located in the same region (Fig. 2). Although the high gain channels of the BATS broadband sensor are saturated in the early stage of this first event, its low gain channels and acceleration sensors completely recorded the whole rupture process (Fig. 3). We combine TWKB and CWB strong motion records in our analysis.
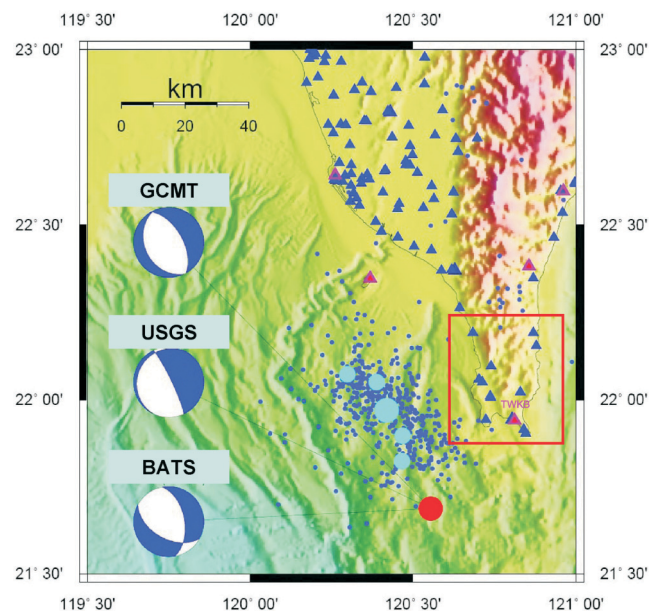

Fig. 2. Locations of the CWB strong motion stations (blue triangle symbols) and BATS stations (purple triangles) recording the Pingtung earthquake. The red dot is the epicenter of the event analyzed in this study. Blue dots are locations of aftershocks (big light-blue dots for major aftershocks). The focal mechanisms are determined by Global CMT, USGS, and BATS, respectively. The seismic data used in this study are from stations inside the array marked by the red rectangle.
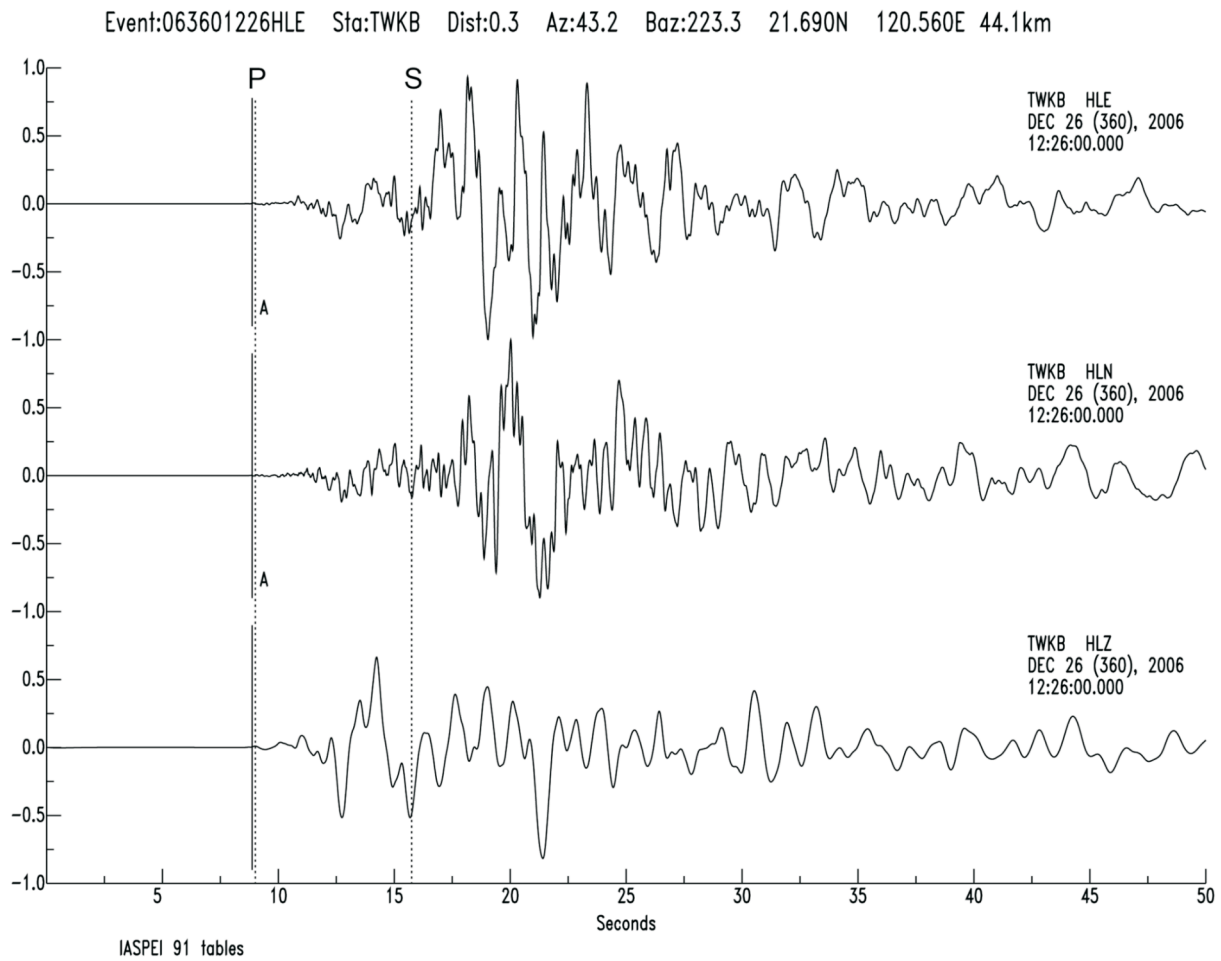
Fig. 3. The three-component acceleration seismograms of the Pingtung earthquake recorded at station TWKB of BATS. Vertical lines indicate the theoretical predictions of arrival times of P and S waves.

Finally, 12 free-field strong motion records for events with epicentral distances of less than 62 km were selected. These strong motion records were obtained from stations that were all close to one another. Figure 4 displays vertical velocity seismograms at different epicentral distances. It was found that all first and latter arrivals in seismograms agree with their epicentral distances. In Fig. 4, each seismogram was integrated from its acceleration waveform after being filtered in a signal period band between 2 and 5 sec, and was individually normalized to highlight the coherence of waveforms. The vertical bar in each seismogram shows its initial P arrival time. In Fig. 4a, amplitudes of onset P waves in seismograms are very small with respect to their latter arrivals. The first large amplitude arrivals were delayed by about 3 sec with respect to origin time. Due to the proximity of stations to one another, the recorded seismograms are quite well correlated. These time-shifted seismograms have a common time base and can reasonably be considered as a single set of dense seismic array observations for future signal processing to detect azimuths and apparent velocities of incoming signals to study fault rupture behavior.

3. ANALYSIS AND RESULTS

To identify the propagation of an earthquake rupture within a fault plane, near source dense array observations can be used to estimate the azimuth of approach and apparent velocity of incoming P waves using beamforming analysis or moving-window slowness analysis (Frankel et al. 1991). This type of analysis has been used previously to map rupture propagation using strong-motion records (Huang 2001), identify approaching waves in two dimensions from the Loma Prieta aftershocks (Frankel et al. 1991), and examine the initial onset of the Lander earthquake (Abercrombie and Mori 1994).

For an incident plane wave, the travel time (t_i) at station i can be written as:

$$t_i = S_x x_i + S_y y_i \qquad (1)$$

The terms S_x and S_y are the horizontal components of slowness, and x_i and y_i are the spatial coordinates of the station. In each time window, we test all values of S_x and S_y from 0 to 0.2 sec km^{-1} at intervals of 0.05 sec. Best-fitting slow-
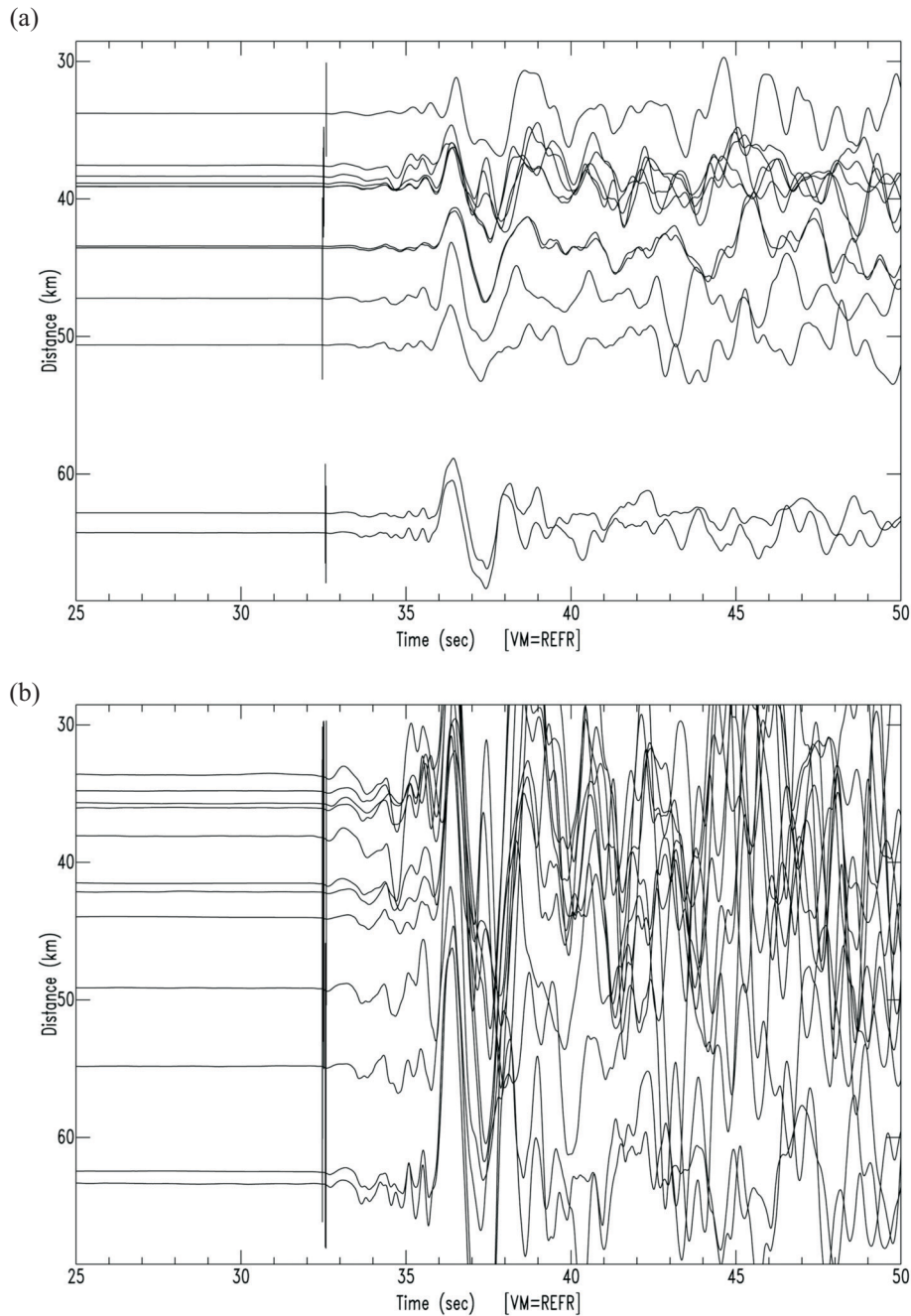
(a)

(b)

Fig. 4. (a). The vertical velocity records (integrated from acceleration) of the Pingtung earthquake from the 12 nearest strong-motion stations on the Hengchun Peninsula. Seismograms are filtered using a signal period band between 2 and 5 sec and individually normalized. They are aligned by an apparent velocity of 8.9 km sec^{-1} and displayed with respect to epicenter distances. The vertical bar in each seismogram shows its initial P arrival time. (b) is the same as (a) with the amplitudes magnified by a factor of 9.

ness was determined by stacking seismic waveforms according to the Nth root stacking method and choosing slowness with the peak value of the stacked trace. We used windows that were 0.5 sec long with a 10% cosine taper on each end, and successive windows were offset by 0.05 sec. Slowness estimates were made for the first 5 seconds before the arrival of S-wave onset as S waves may disturb recordings of the incoming P wave. We used vertical compo-

nent velocity seismograms integrated from one broadband low gain record (station TWKB) and 11 CWB strong motion network acceleration records as array input. From the slowness estimate, the incoming azimuth of the wave is:

$$\Phi = \arctan (S_x / S_y) \qquad (2)$$

and the apparent velocity is:

$$V_a = 1/(S_x^2 + S_y^2)^{1/2} \qquad\qquad (3)$$

In this study, for lack of absolute timing of some strong motion records, we fixed the first arrivals from the hypocenter at a depth of 44 km (reported by CWBSN) as the initial location of the finite rupture plane.

The results for the azimuth and apparent velocity of incoming signals for the various time windows are shown as slowness maps in Figs. 5 and 6, respectively. The great circle in each figure shows the apparent velocity of major seismic energy approaching this array and the white dot indicates the location of the peak value. The red area in each map represents the slowness region for 90% energy concentration of incident waves. In Fig. 5, the slowness maps show initial onset at the fixed location of the hypocenter, which continues for at least 0.3 seconds. After that, the energy spot on the slowness map splits into two groups. One group stays at the same azimuth and apparent velocity, while the other moves southward with smaller apparent velocity (Fig. 6a). It

is evident that the initial onset begins to extend its rupture southward toward the shallower portion of the fault plane. However, the southward extension did not continue. At 1.3 seconds after the initial onset, we observed a new energy spot arising in a northerly direction with a larger apparent velocity than the initial onset (Fig. 6b). This observation has the rupture extending northward toward the deeper portion of the fault plane. Following this initial rupture process, large amplitudes, evidently from a major rupture of this event, are found on array seismograms (Fig. 4) and analyzed slowness diagrams.

Although direct source information from the above analysis provides insight into source rupture behavior within a fault plane, detailed source rupture processes cannot be constructed for future estimation. To image the initial source rupture process of this earthquake, we use an approach similar to that of Ishii et al. (2005) for locating the source rupture process of the 2004 Sumatra-Andaman earthquake at a teleseismic distance. In principle, our analysis utilizes
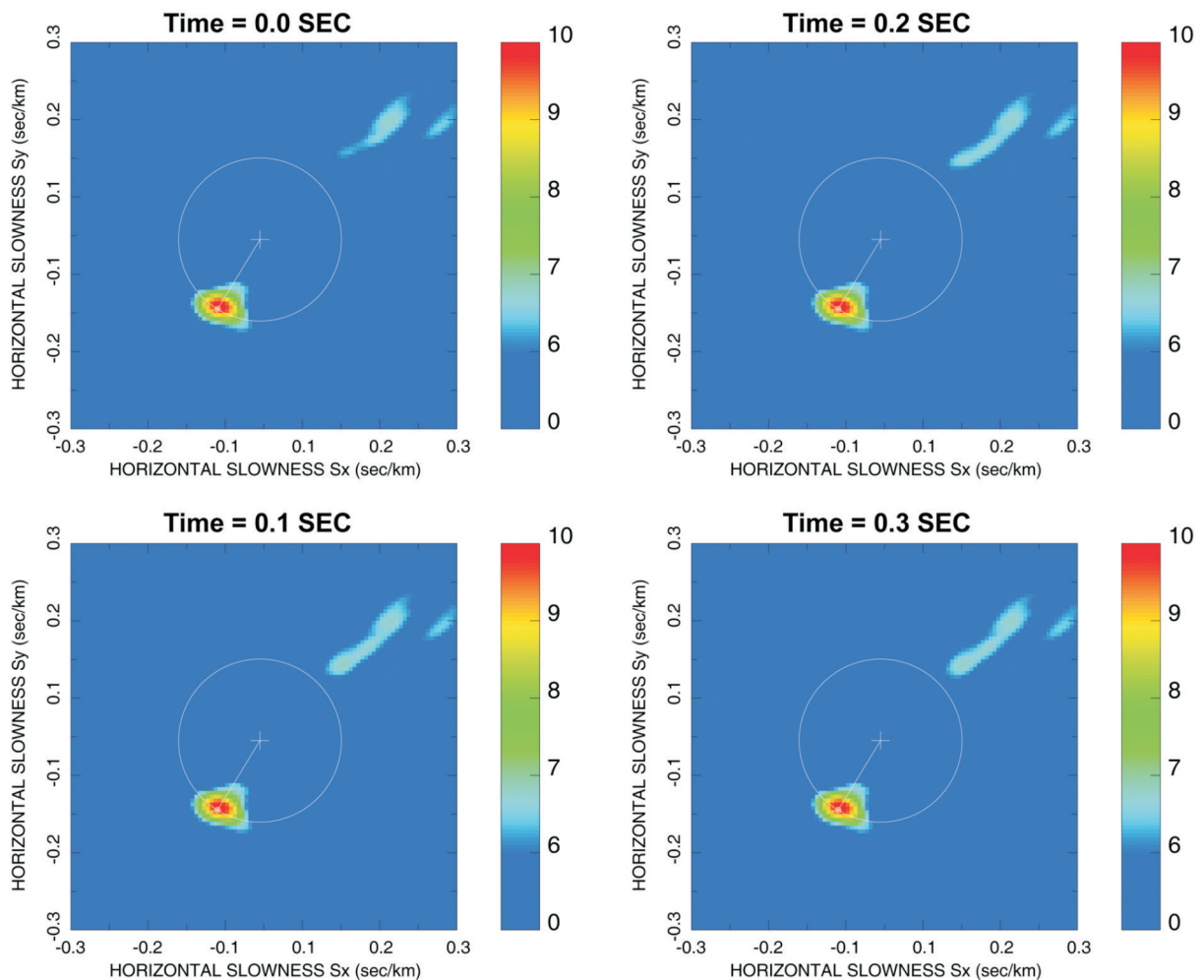

Fig. 5. Stacking beam amplitude as a function of slowness for four windows in the initial onset of the P-wave train. S_x and S_y are the slowness of the assumed ray in the east and north directions, respectively. The circle denotes constant value of apparent velocity of the incoming wave. The dot denotes the peak of the true slowness. The line between the cross and dot shows the azimuth of the incident wave.
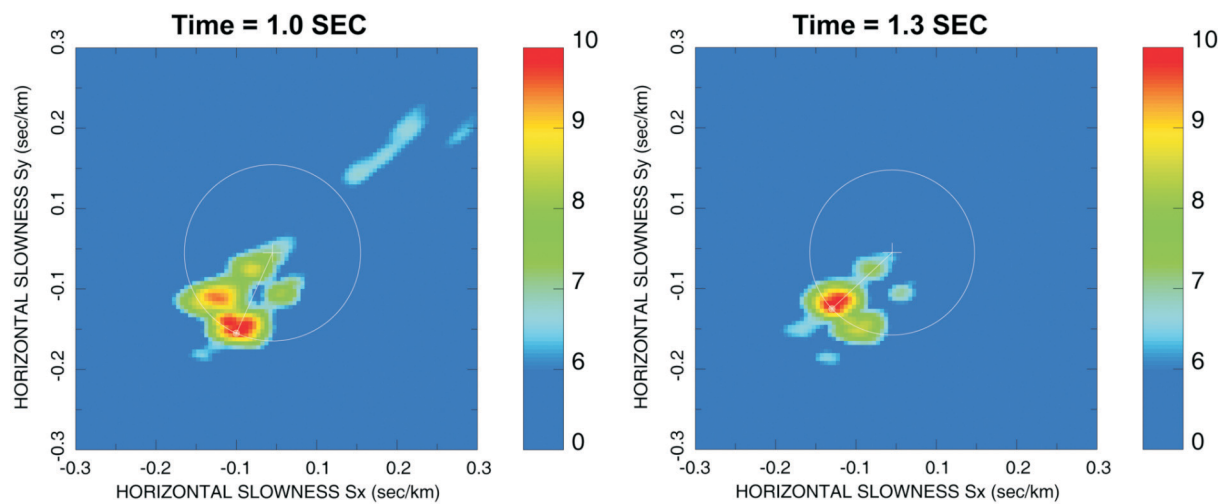
Fig. 6. Stacking beam amplitude for time windows of 1.0 and 1.3 sec after the initial onset of the Pingtung earthquake. Both diagrams show the slowness peak moves in the south and north directions and consequently indicate the rupture propagates southward and northward along the fault plane.

back-projection mapping in which seismograms are stacked for each possible source location to obtain a direct image of the source (Ishii et al. 2005). The stacking procedure sums the energy that is radiated from a given source point, and cancels out other energies present in the seismograms. The resulting stacked images, as functions of time and position of each potential source location, provide an estimate of the relative intensity of radiated seismic energy at all source locations and times. The source imaging procedure has been well examined in our previous analysis for earthquake relocation (Huang 2008). In this study, information on fault planes (strike, dip, and slip) from USGS and regional velocity model from Chen (1995) has been employed to construct source rupture. The near vertical and eastern dip fault plane of the UGSG CMT solution was selected as the rupture plan for source imaging. A series of array seismograms of 0.3 sec long prior to initial P arrivals and 0.2 sec long following the arrivals were selected to map seismically radiated energy snapshots within the fault plane. The selected images are shown in Fig. 7 at progressive times. Time zero is the earthquake's initial onset at the hypocenter lasting approximately 0.3 seconds. Thereafter, the rupture extends toward the deeper northern portion of the fault plane. In the final stage of initial onset, there was small continuous slip with northward propagation up to about one second. At the end of this initial onset, major slip occurred north of the hypocenter.

4. DISCUSSION AND CONCLUSIONS

The 2006 Pingtung earthquake of 1226 UTC is one of a few large intermediate depth earthquakes to have occurred in the offshore region of southwestern Taiwan. Analysis of such event provides a better understanding of the mecha-

nisms of deep intraplate events and associated seismic hazard. Although information on such intraplate events has been previously limited primarily to seismic observations, one of a few well recorded large intermediate depth normal-faulting earthquakes was the 2001 Nisqually earthquake, which occurred at a depth of 50 - 60 km within the subducting Juan De Fuca plate in the Cascadia Subduction zone; its surface deformation was well mapped by the Global Positioning System (GPS) (Bustin et al. 2004). Fault parameters of the Nisqually earthquake were well determined from regional moment tensor solutions and the near source surface deformation recorded by GPS. However, understanding of rupture behavior for this earthquake was lessened by the lack of near source seismic data. The Pingtung earthquake is the first intermediate depth event for which surface deformation and near source ground motions were well recorded by GPS and a dense strong-motion array.

Our array analysis captures the emergent onset of fault rupture for the Pingtung earthquake. We suggest that initially there was a small-scale fault rupture of ~0.3 sec in concordance with the hypocenter causing fault slip to extend southward along the shallower portion of the fault plane; after which, a rupture front propagated both northward and downward. Following this small-scale initial slip, a major rupture occurred (Figs. 5, 6). Furthermore, information regarding the spatial variation of the onset rupture has been obtained by a backward projection of array seismograms to image the source rupture within the fault plane (Fig. 7). Temporal rupture behavior of this event was revealed using the beamforming method. The rupture process is interpreted as being one of a rapid extension after initial smooth growth. Thereafter, rupturing continued northward before a major rupture occurred at approximately 3 sec after initial onset.

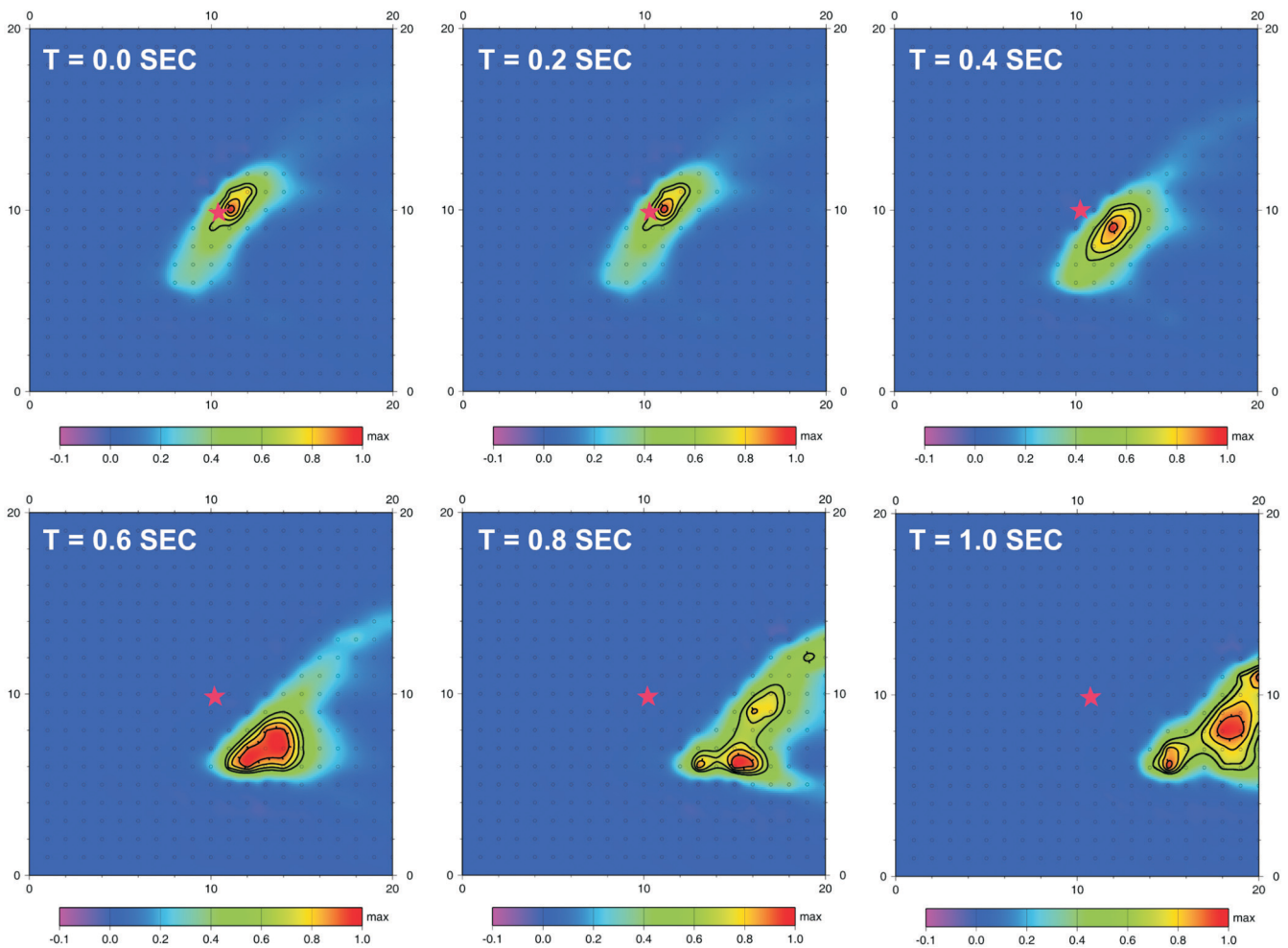The rupture processes of an earthquake's onset are of

Fig. 7. Maps showing the distribution of energy radiation on the fault plane at 0.2-sec intervals following the initiation of the Pingtung earthquake. The red star denotes the hypocenter. The fault plane is a 20 × 20 km square area surrounding the hypocenter.

great interest to earthquake science. Currently, two end-member models of earthquake nucleation, a pre-slip model and a cascade model, have been proposed to describe the behavior of earthquake rupture in its initial stage, and both are still subject to debate (Abercrombie 2005). In the pre-slip model, small and isolated sub-events may result from slow aseismic slip in a nucleation zone and pre-slip eventually causes the mainshock. The cascade model has no zone of aseismic pre-slip. The beginning of a large earthquake is no different from the beginning of a small earthquake. In the case of a pre-slip earthquake model, the final magnitude would be related to the nature of the nucleation process, and seismograms of large earthquakes would look different from those of smaller earthquakes from the outset. The different beginnings of small and large earthquakes may allow the final size of the earthquake to be predicted before the fault stops moving.

The Pingtung earthquake is not the first event analyzed in the study of the rupture behavior of such an emergent onset. Previous studies from the 1989 California Loma

Prieta earthquake (Wald et al. 1991) and 1992 California Landers earthquake (Abercrombie and Mori 1994) have discussed the dynamic processes of earthquake rupture beginnings. The onset of the Loma Prieta earthquake had an initial rupture process, with a 2.5-sec delay between the origin time and the onset of the main energy release. There is some evidence that its early rupture was very smooth, radiating relatively little high-frequency energy (Ellsworth 1992). Similarly, the onset of the Landers earthquake was emergent. The first large amplitude arrivals were delayed by about 3 sec with respect to origin time. That earthquake began with two subevents, an M_w 4.4 followed by an M_w 5.6 shock, preceding the main energy release (Abercrombie and Mori 1994); however, both subevents do not appear anomalous in frequency content in comparison to simple moderate-sized earthquakes. There was no apparent lack of high frequencies radiated by these early subevents and no evidence for anomalous long-period energy. Analysis from those two events implies different origins of earthquake faulting in their initial stages. Analysis for the Landers earthquake suggests

that the early subevents were normal events that just triggered or grew into a much larger earthquake. However, analysis for the Loma Prieta earthquake indicates that the rupture behavior of its initial onset was something different from the main energy release.

In sum, this analysis of the Pingtung earthquake has provided more detailed spatial information for a fault rupture in its initial stage than in previous studies. It seems to indicate the behavior of a seismic nucleation zone, thus a region of initial rupture (hypocenter) and its smooth growth (slow aseismic slip), before the major fault rupture occurs (Figs. 4, 5). However, presently available evidence does not permit a confident statement on whether the onset of the major slip of the Pingtung earthquake was the result of the pre-slip. One of the reasons is that the rupture fault plane of this event and the regional velocity model are still not well constrained. Moreover, assuming the fault rupture plane based on the USGS focal mechanism and may induce some errors in the source imaging and the interpretation of the initial rupture. Herein, we conclude that analysis of the initial onet of the Pingtung earthquake seems to support the pre-slip model; however, uncertainties still remain and cascade beginnings for the earthquake rupture process cannot be totally ruled out. Future analysis for frequency content of the initial onset and its stress drop would be useful in verifying the origin of initial onset.

REFERENCES

Abercrombie, R. E., 2005: The start of something big? *Nature*, **438**, 171-173.

Abercrombie, R. E. and J. Mori, 1994: Local observations of the onset of a large earthquake: 28 June 1992 Landers, California. *Bull. Seismol. Soc. Am.*, **84**, 725-734.

Bustin, A., R. D. Hyndman, A. Lambert, J. Ristau, J. He, H. Dragert, and M. Vand der Kooji, 2004: Fault parameters of the Nisqually earthquake determined from moment tensor solutions and the surface deformation from GPS and InSAR. *Bull. Seismol. Soc. Am.*, **94**, 363-376.

Chen, Y. L., 1995: Three-dimensional velocity structure and kinematic analysis in the Taiwan area. Master Thesis, National Central University, Chung-Li, Taiwan, ROC.

Choy, G. L. and J. W. Dewey, 1988: Rupture process of an extended earthquake sequence: Teleseismic analysis of the Chilean earthquake of March 3, 1985. *J. Geophys. Res.*, **93**, 1103-1118.

Ellsworth, W. L., 1992: Imaging fault rupture without inversion. *Seismol. Res. Lett.*, **63**, 73.

Frankel, A., S. Hough, P. Friberg, and R. Busby, 1991: Observations of Loma Prieta aftershocks from a dense array in Sunnyvale, California. *Bull. Seismol. Soc. Am.*, **81**, 1900-1922.

Goldstein, P. and R. J. Archuleta, 1991: Deterministic frequency-wavenumber methods and direct measurements of rupture propagation during earthquakes using a dense array: Data analysis. *J. Geophy. Res.*, **96**, 6187-6198.

Haessler, H., A. Deschamps, H. Dufumier, H. Fuenzalida, and A. Cisternas, 1992: The rupture process of the Armenian earthquake from broad-band teleseismic body wave records. *Geophys. J. Int.*, **109**, 151-161.

Huang, B. S., 2000: Two-dimensional reconstruction of the surface ground motions of an earthquake: The September 21, 1999, Chi-Chi, Taiwan earthquake. *Geophys. Res. Let.*, **27**, 3025-3028.

Huang, B. S., 2001: Evidence for azimuthal and temporal variations of the rupture propagation of the 1999 Chi-Chi, Taiwan Earthquake from dense seismic array observations. *Geophys. Res. Let.*, **28**, 3377-3380.

Huang, B. S., 2008: Tracking the North Korea nuclear explosion on October 9, 2006 using the Hi-Net array and FORMOSAT-2 observation satellite. *Phys. Earth Planet. Inter.*, **167**, 34-38, doi: 10.1016/j.pepi.2008.02.004.

Ishii, M., P. M. Shearer, H. Houston, and J. E. Vidale, 2005: Extent, duration and speed of the 2004 Sumatra-Andaman earthquake imaged by the Hi-net array. *Nature*, **435**, 933-936.

Liu, K. S., T. C. Shin, and Y. B. Tsai, 1999: A free-field strong motion network in Taiwan: TSMIP, *Terr. Atmos. Ocean. Sci.*, **10**, 377-396.

National Disaster Prevention and Protection Commission, ROC, 2007: Statistics on the losses on natural disaster, http://www.ndppc.nat.gov.tw/.

Shin, T. C., 1993: Progress summary of the Taiwan strong motion instrumentation program, Symp. on the Taiwan strong motion instrumentation program, 1-10.

Wald, D. J., T. H. Heaton, and D. V. Helmberger, 1991: Rupture model of the 1989 Loma Prieta earthquake from the inversion of strong motion and broadband teleseismic data. *Bull. Seismol. Soc. Am.*, **81**, 1540-1572.

Wessel, P. and W. H. F. Smith, 1995: A new version of the Generic Mapping Tools (GMT), *EOS Trans. AGU*, **76**, 329.